Regular Article

blood

RED CELLS, IRON, AND ERYTHROPOIESIS

Eltrombopag: a powerful chelator of cellular or extracellular iron(III) alone or combined with a second chelator

Evangelia Vlachodimitropoulou,[1] Yu-Lin Chen,[2] Maciej Garbowski,[1] Pimpisid Koonyosying,[1] Bethan Psaila,[3] Martha Sola-Visner,[4] Nichola Cooper,[5] Robert Hider,[2] and John Porter[1]

[1]Haematology Department, University College London, London, United Kingdom; [2]Institute of Pharmaceutical Science, King's College London, London, United Kingdom; [3]MRC Weatherall Institute of Molecular Medicine, John Radcliffe Hospital, University of Oxford, Oxford, United Kingdom; [4]Paediatrics Department, Boston Children's Hospital, Boston, MA; and [5]Haematology Department, Hammersmith Hospital, Imperial College London, London, United Kingdom

Key Points

- ELT is a powerful iron chelator, mobilizing iron and ferritin, reducing ROS, and restoring insulin production at clinically achievable levels.
- ELT enhances cellular iron chelation when combined with clinically available iron chelators through the shuttling of iron(III).

Eltrombopag (ELT) is a thrombopoietin receptor agonist reported to decrease labile iron in leukemia cells. Here we examine the previously undescribed iron(III)-coordinating and cellular iron-mobilizing properties of ELT. We find a high binding constant for iron(III) (log β_2=35). Clinically achievable concentrations (1 μM) progressively mobilized cellular iron from hepatocyte, cardiomyocyte, and pancreatic cell lines, rapidly decreasing intracellular reactive oxygen species (ROS) and also restoring insulin secretion in pancreatic cells. Decrements in cellular ferritin paralleled total cellular iron removal, particularly in hepatocytes. Iron mobilization from cardiomyocytes exceeded that obtained with deferiprone, desferrioxamine, or deferasirox at similar iron-binding equivalents. When combined with these chelators, ELT enhanced cellular iron mobilization more than additive (synergistic) with deferasirox. Iron-binding speciation plots are consistent with ELT donating iron to deferasirox at clinically relevant concentrations. ELT scavenges iron citrate species faster than deferasirox, but rapidly donates the chelated iron to deferasirox, consistent with a shuttling mechanism. Shuttling is also suggested by enhanced cellular iron mobilization by ELT when combined with the otherwise ineffective extracellular hydroxypyridinone chelator, CP40. We conclude that ELT is a powerful iron chelator that decreases cellular iron and further enhances iron mobilization when combined with clinically available chelators. (*Blood*. 2017;130(17):1923-1933)

Introduction

Eltrombopag (ELT) is an orally bioavailable small molecular thrombopoietin receptor (TPO-R) agonist approved for the treatment of idiopathic thrombocytopenia and thrombocytopenia associated with chronic hepatitis C. An underappreciated property of ELT is its binding to metal ions, and in particular to iron(III). Oral consumption of ELT with calcium-, aluminum-, and magnesium-containing foods reduced absorption of these metals,[1,2] which could be a result of chelation of metal ions.[1] ELT also decreased labile iron within leukemia cells,[3] which could be relevant to its antiproliferative and apoptotic effects in acute myeloid leukemia,[3,4] as well as the treatment of hepatocellular carcinoma.[5] In principle, some beneficial effects on hematopoiesis in myelodysplastic syndrome[6] and aplastic anemia[7,8] could also derive from iron chelation. Our preliminary findings suggested low ELT concentrations could mobilize cellular iron.[9,10] ELT might therefore have a role in treating iron overload conditions, either alone or when combined with clinically licensed chelators. However, little is known about the iron-binding properties of ELT. Unknowns include the iron coordination mechanism, iron(III)-binding constant, effects on iron-induced reactive oxygen species (ROS), effects on storage iron, relative interaction with different cell types, and mechanisms of interaction with other chelators.

Iron chelation therapy is used to treat transfusional iron overload in thalassemias, sickle cell disease, and myelodysplastic syndrome. Nontransfusional iron overload may also be treated with iron chelation. Although 3 iron chelators are now licensed, the removal of excess iron is slow, and treatment can also be limited by chelator toxicity, particularly at higher doses. Therefore, combinations of chelators have been used to enhance chelation. Although simply additive effects can be useful, true synergism, in which 1 chelator increases the rate of access of a second chelator to iron pools, would be valuable.[11]

The ability of an iron chelator to mobilize cellular iron is related to the iron-binding constant and the ability of the iron chelator to enter cells.[11] Thus, chelators with low lipid solubility or large molecular weight enter cells slowly and have little effect on iron release.[12] These same properties also affect iron release in animal models,[13] as well as affecting their access to intracellular iron pools,[14] including metalloenzymes,[15,16] cell cycle, growth,[17] and apoptosis.[18]

Submitted 13 October 2016; accepted 22 July 2017. Prepublished online as *Blood* First Edition paper, 1 September 2017; DOI 10.1182/blood-2016-10-740241.

The online version of this article contains a data supplement.

The publication costs of this article were defrayed in part by page charge payment. Therefore, and solely to indicate this fact, this article is hereby marked "advertisement" in accordance with 18 USC section 1734.

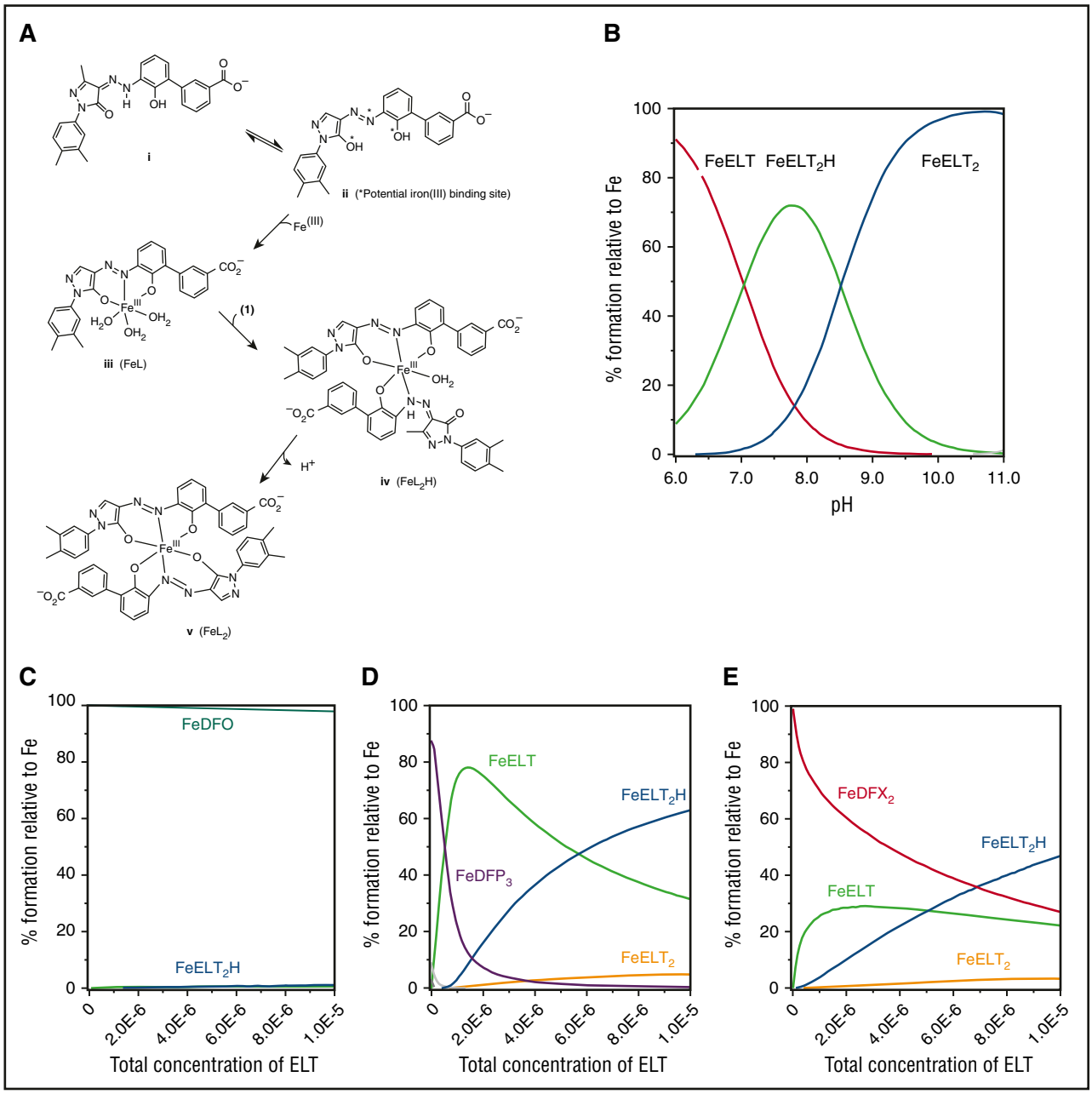

Figure 1. Structure and iron-binding properties of ELT. Data on the iron-binding properties of ELT were obtained specifically for this article and are not previously published elsewhere. The iron-binding properties of other chelators are based on previously published data.[11,19] (A) Structure of ELT and its iron complexes are shown. The free ligand possesses 2 tautomers (i and ii). Three major iron(III) complexes have been identified: iii (FeELT), iv ($FeELT_2H$), and v ($FeELT_2$). (B) The speciation of iron(III) in the presence of ELT as a function of pH. $[Fe]_{total}$=1 μM; $[ELT]_{total}$=10 μM is shown at steady state (ie, when sufficient time has elapsed for the reactions to go to completion). These proportions are calculated from the iron-binding constants for iron-chelate complexes of the respective chelators shown in Table 1 and determined as described in "Materials and methods." Titration with iron(III) yielded 3 equilibrium constants: K_{FeL}=25.6, K_{FeL2H}=43.4, and K_{FeL2}= 34.9. ELT has 3 pK_a values (the pH at which half the molecules are ionized) of 2.6, 8.7, and 11.1. Using these data, a pFe value of 22.0 (the strength of iron(III) binding, being the negative log of the unbound iron(III) concentration under defined conditions (1 μM iron[III] and 10 μM chelator[10]) was determined, which is greater than that of DFP (20.4) and very similar to that of DFX (23.1). Competition between ELT and other chelators for iron(III) are shown for (C) 1 μM DFO, (D) 3 μM DFP, and (E) 2 μM DFX. These show the predicted proportions of each ELT iron complex when mixed with a second chelator, after reactions have gone to completion (in steady state). Thus, for example, at 1 μM ELT, more than 99% of iron(III) will be bound to DFO (C), whereas under the same conditions, about half the iron will be bound to DFP (D), and about 70% to DFX (E).

The 2 largest chelatable iron pools are, first, within hepatocytes where more than 70% of body iron is deposited and, second, iron released from macrophages after the catabolism of red cells.[19] The most rapidly chelatable iron pool within cells is the so-called labile iron pool (LIP), which is relatively small at any moment and is predominantly contributed to by intracellular ferritin catabolism.[19,20]

In this article, we investigated the iron-binding properties of ELT and its ability to mobilize intracellular iron and to decrease ROS-mediated cellular damage, using a recently described cell culture model.[11] Chelators can be metabolically inactivated at their iron-binding sites (particularly in hepatocytes, but with wide interspecies variability), where metabolism in rodents, and hence chelator efficacy, can differ significantly from humans.[21,22] In vitro screening therefore ideally needs

to include human-derived cells. We have included a human hepatoma cell (HuH7) as the primary screen, as drug metabolism is well described and has the advantage of stability in culture, whereas primary cells can lose key metabolism enzymes within hours of isolation. Iron overload in myocardium and the endocrine system is quantitatively much smaller than in the liver, but damage is clinically important, causing fatal cardiomyopathy and type 1 diabetes, respectively. We have therefore also investigated cell lines derived from these cells. Decrements in total cellular iron and ferritin induced by ELT have been compared with clinically licensed chelators. We have also examined whether ELT diminishes iron-induced intracellular ROS, and thereby restores cell function. We have investigated whether additional iron chelation can be achieved by combining ELT with other chelators and examined the mechanisms by which this occurs.

Materials and methods

Spectrophotometric method for pK_a and iron stability constant

An automated titration system[20] was used under the conditions of constant temperature at 25°C and constant ionic strength at 0.1 M, using 0.1 M KCl, 0.1 M HCl, and 0.1 M KOH. The pH electrodes were calibrated using the GLEE program.[23] The titration data were analyzed using the pHab program.[24] Species plots were calculated using the HYSS program.[25] Analytical grade reagent materials were used in all solutions.

Determination of kinetics of iron binding to ELT, DFX, and CP40

These were performed spectrophotometrically, using difference spectra where necessary, with a Varioscan Flash plate reader (UK). Kinetic data were plotted using absorbance for ELT or deferasirox $(DFX)_2Fe$ complexes. Wavelengths chosen for kinetic analysis were determined from spectral plots of ELT, DFX, and their respective iron complexes. Buffered ferric citrate was prepared[26] using concentrated 4-morpholinepropanesulfonic acid pH 7.4. ELT was prepared as a 1% solution in dimethyl sulfoxide (DMSO). ELT–iron complexes were prepared as follows: ELT/DMSO aliquot was mixed with ferric chloride atomic standard solution added at desired molar ratios. pH was increased by adding 1 M 4-morpholinepropanesulfonic acid at pH 7.4. Deferasirox 1% solution was prepared in DMSO. ELT in culture media was diluted to ensure final concentration of DMSO less than 1%.

The cellular models and iron measurements

The human hepatocarcinoma (HuH7) and rat cardiomyocyte (H9C2) cell lines were purchased from Sigma-Aldrich UK. RINm5F rat pancreatic cell line, which secretes insulin after a glucose challenge, was from LGC ATCC Sales, UK. H9C2 and HuH7 cells were plated, cultured, and iron-loaded, as recently described.[9,11] Iron loading was obtained by serially treating cells with 10% fetal bovine serum (FBS)-RPMI media over the course of two 10-hour periods. Increments in cellular iron differed between cell types (3-fold in HuH7, 2-fold in H9C2, and 4-fold in RINm5F cells). Cell washing, chelator exposure, and measurement of cellular iron using ferrozine assay, adjusted for cellular protein, was as described.[11] Iron release was performed in serum-free medium, as FBS contained free iron that bound chelators extracellularly, decreasing efficacy. Reports of ELT inhibition by serum[4] are more likely a consequence of iron contamination in FBS than protein binding to ELT (supplemental Data, available on the *Blood* Web site).

Cell damage and viability was assessed using the LDH Cytotoxicity Detection Kit (Takara Bio Inc). Human and rat tissue ferritin of cell lysates were measured by enzyme-linked immunosorbent assay kits (Cusabio, Wuhan, China; and My BioSource, San Diego, CA, respectively). Desferrioxamine (DFO), deferiprone (DFP), and DFX were purchased from Sigma-Aldrich UK, and ELT from Generon, UK.

Table 1. Comparison of the structure and iron-binding properties of ELT and other chelators

	DFO	DFP	DFX	ELT
Molecular weight	561	139	373	442
Chelator/iron(III) ratio	1:1	3:1	2:1	2:1 and 1:1
Log stability constant for iron (III)	30.6	37.2	36.5	34.9
pFe (pmol/L)	26.6	20.7	23.1*	22.0
Charge of free ligand at pH 7.4	1+	0	1−	1−
Charge of iron complex at pH7.4	1+	0	3⁻	3⁻ (2:1); 0 (1:1)
Lipid solubility free ligand (log P)	−3	−0.8	4.3	6.3

Binding properties of ELT are not previously described and were determined specifically for this article. The relative stabilities of iron(III) binding are represented by the pFe, where the pFe of a given chelator for iron(III) is the negative log of the uncoordinated metal concentration under defined conditions.[50] The higher the pFe values, the lower the concentration of uncoordinated iron(III), and hence the greater stability for the iron–chelate complex. ELT can form neutrally charged 1:1 complexes with iron(III) or 3− negatively charged 2:1 complexes. Properties of other chelators use published data,[11,19] except for the pFe value of DFX, where 23.1 is used based on the properties of the molecule in 100% water; The widely adopted values of 22.4 or 22.5 are based on titrations run in 20% DMSO. When pairs of chelators are combined in solution, iron(III) will bind preferentially to the chelator with the higher pFe value. This is highest for DFO and lowest for DFP, with DFX having an intermediate value but greater than ELT.

Kpart, partition coefficient.[51-53]

*Value determined for 100% aqueous system.

Detection of reactive oxygen species

A cell-permeable oxidation-sensitive fluorescent probe 5,6-carboxy-2′,7′-dichlorofluoresceindiacetate (DCFH-DA; Molecular Probes, Leiden, Netherlands) was used, where nonfluorescent DCFH-DA is hydrolyzed to DCFH inside of cells, yielding highly fluorescent DCF in the presence of intracellular hydrogen peroxide (H_2O_2). Cells plated in Corning 24-well plates (Sigma-Aldrich, Haverhill, MA) were preincubated with 4 mM DCFH-DA for 30 minutes at 37°C. Chelators were then added, and fluorescence was recorded continuously over the course of 90 minutes (excitation at 504 nm, emission at 526 nm). The time between the addition of chelators and commencing ROS recording was 3 to 5 minutes.

Insulin quantification

After iron loading and chelator treatment, the cells were challenged with Krebs' Ringer buffer twice, for 1 hour at a time, containing 2.8 mM and 16.7 mM glucose.[27,28] The supernatant was then collected and insulin concentration determined using a standard rat insulin enzyme-linked immunosorbent assay kit (Life Technologies Limited, UK).

Results

Iron(III)-binding and speciation plots for ELT alone or combined with other chelators

The previously undescribed iron(III)-binding properties of ELT are key to understanding the effect on cellular iron mobilization, either alone or when combined with other chelators. The iron-binding properties of ELT in Figure 1 and Table 1 were determined specifically for this communication. The log *P* value of ELT was derived from a computer program.[29] The usual chemical representation of ELT is shown in structure 1, lacking a high-affinity iron(III)-binding site (Figure 1A). However, ELT can be represented as a mixture of 2 tautomers, with the second (Figure 1Aii) possessing a potential tridentate iron(III)-binding site. The 1:1 complex (Figure 1Aiii) possesses zero net charge (Table 1) and has a molecular weight less than 500, similar to the DFP–iron complex. The speciation plot for iron(III)/ELT (Figure 1B) indicates a mixture of the 1:1 and 2:1 complexes at pH 7.4. Figure 1C-E shows speciation plots of iron(III) (1 μM) binding at increasing

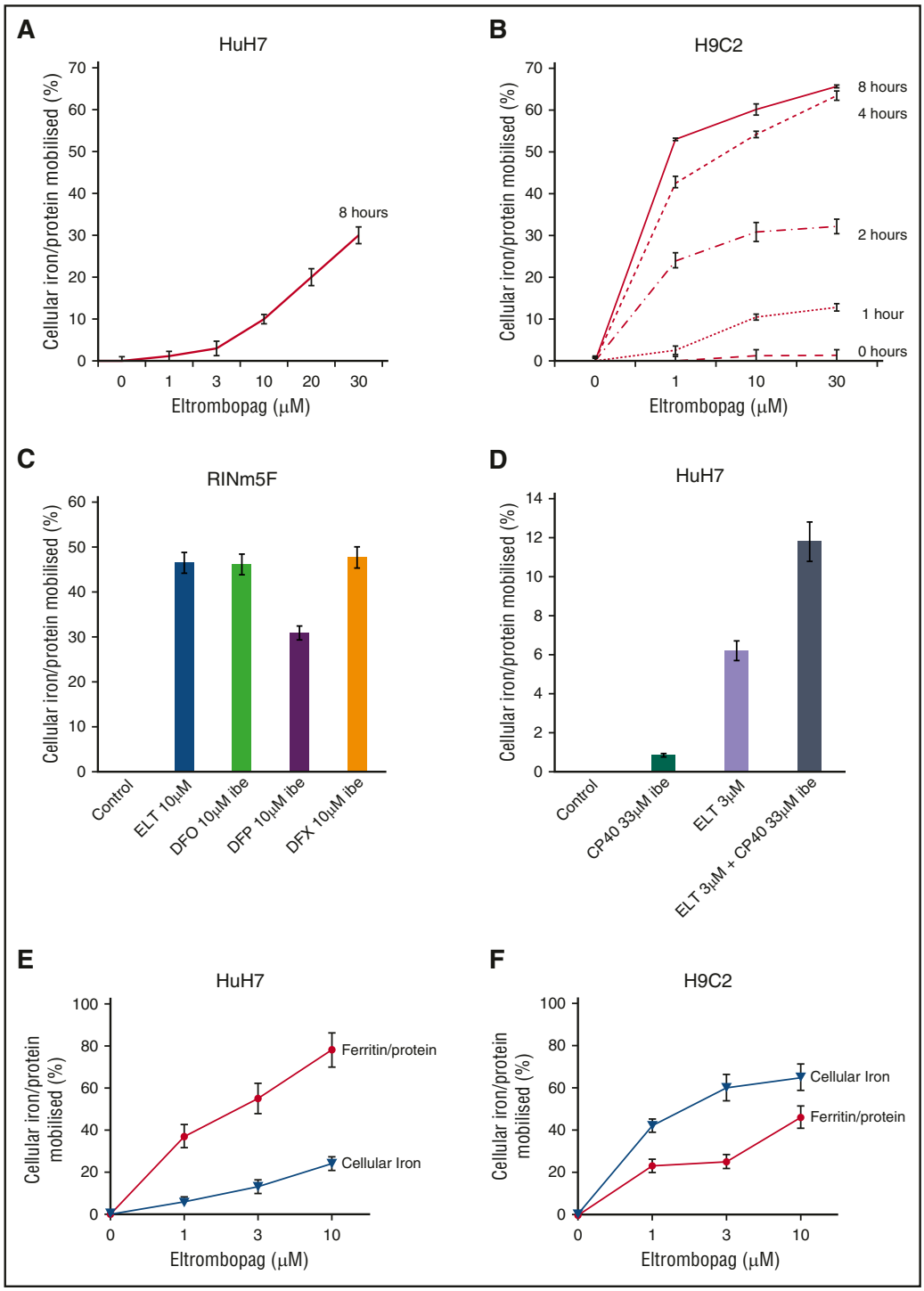

Figure 2. Cellular iron mobilization and/or ferritin iron decrements with ELT from HuH7, H9C2, and RINm5F cells. (A) Dose response for iron release from HuH7 cells at 8 hours is shown. (B) Dose response for iron release from H9C2 cells at 1, 2, 4, and 8 hours is shown. Cells were loaded with iron, as described in "Materials and methods." Adherent cells were rinsed 4 times, including 1 wash containing DFO at 30 μM IBE and 3 PBS washes, and subsequently exposed to ELT and other chelators for the times shown. Chelator-containing supernatants were then removed, and the cells washed 4 times as described before lysing with 200 mM NaOH. Intracellular iron concentration was then determined at each point, using the ferrozine assay described in "Materials and methods" and normalized for total cellular protein in each well. Results shown are expressed as the percentage of T_0 cellular iron released at the times shown and are the mean ± SEM of 6 replicates in 1 representative experiment. (C) Iron release by ELT 10 μM and DFO, DFP, and DFX 10 μM IBE after 8 hours of treatment in RINm5F cells and (D) iron release by ELT, CP40 and a combination of ELT and CP40 in HuH7 cells. Cells were iron-loaded using two 10-hour changes of 10% FBS-containing RPMI media and rinsed as above. Comparison of the effect of ELT on ferritin and total cellular iron mobilization in (E) HuH7 hepatocyte and (F) H9C2 cardiomyocyte cells is shown. After iron loading, chelator treatment for 8 hours, and rinsing, iron content was ascertained as described earlier. Ferritin was quantified using commercially available enzyme-linked immunosorbent assay kits appropriate for our rat and human cell lines. Results are expressed as the percentage of T_0 cellular iron mobilized or decrement of ferritin expressed as percentage of T_0 values at the times shown and are the mean ± SEM of 3 replicates of 1 representative experiment.

Table 2. Comparison of percentage of intracellular iron mobilized at 8 hours in a cardiomyocyte (H9C2) and a hepatocyte (HuH7) cell lines by clinically available chelators or ELT, alone or in combination

	H9C2 cardiomyocyte-like cells	HuH7 hepatocyte-like cells
DFO 1 μM IBE	14.2 ± 1.2	28.6 ± 1.4
DFP 1 μM IBE	17.1 ± 1.5	25.7 ± 1.2
DFX 1 μM IBE	11.7 ± 1.0	22.8 ± 1.7
ELT 1 μM	42.1 ± 2.1	6.9 ± 0.3
ELT 1 μM + DFO 1 μM IBE	58.2 ± 2.5	34.3 ± 1.1
ELT 1 μM + DFP 1 μM IBE	59.9 ± 3.1	38.2 ± 1.5
ELT 1 μM + DFX 1 μM IBE	66.4 ± 2.4	51.4 ± 1.9

Chelator concentrations are expressed as IBE. Cells were preloaded with iron, rinsed, and incubated with chelators, and cellular iron was determined as described in Figure 2. Results shown as the percentage iron released expressed as a percentage of T_0 cellular iron and are the mean ± SEM of 4 replicates in 1 experiment percentage iron release after 8 hours of chelator treatment.

concentrations of ELT (1-10 μM) in the presence of DFO 1 μM, DFP 3 μM, and DFX 2 μM. These predict proportions of iron bound to ELT or a second chelator, after reactions have proceeded to completion. Thus, for example, at 1 μM ELT, more than 99% of iron(III) will be bound to DFO (Figure 1C), whereas about half of the iron will be bound to DFP (Figure 1D), and about 70% to DFX (Figure 1E). These values are helpful in interpreting iron-release studies using combinations of ELT with a second chelator, but do not predict the rates at which reactions proceed.

ELT decreases cellular iron in cardiomyocyte and hepatocyte cell lines

Mobilization of total cellular iron from HuH7 cells was examined between 1 and 30 μM ELT at 8 hours (Figure 2A). These are clinically relevant, as C_{max} plasma concentrations of 8, 18, and 28 μM have been reported at 30, 50, and 75 mg/day.[30] In cardiomyocytes, as little as 1 μM ELT achieved significant mobilization after only 1 hour (Figure 2B). A 2:1 binding of ELT to iron(III) (Figure 1 and Table 1) implies 0.5 μM iron-binding equivalents (IBE) at 1 μM ELT. Comparison of iron mobilization by 1 μM ELT with DFP, DFO, and DFX in HuH7 or H962 cardiomyocytes is shown in Table 2 (top 4 rows). In HuH7, ELT was less effective than DFP, DFX, and DFO at 1 μM. In contrast to the lower efficacy of ELT than other chelators in HuH7 cells, 1 μM ELT mobilized more iron than DFO, DFX, or DFP in H9C2 cells (Table 2). The relevance of ELT metabolism to its relative efficacy in HuH7 and H962 is discussed here.

As cell viability could influence iron release independent of chelation, experiments were only performed where baseline viability exceeded 98%, as assessed by the LDH assay. Hepatocytes showed no signs of toxicity after 8 hours of ELT treatment, up to 30 μM. In contrast, cardiomyocyte viability after 8 hours of exposure to 30 μM ELT fell to 93%. Thus, some iron release in cardiomyocytes at 30 μM (Figure 2B) could be partially attributed to toxicity.

ELT decreases cellular ferritin

We next wished to determine how changes in total cellular iron were paralleled by changes in cellular ferritin. When cells were iron-loaded (see "Materials and methods"), tissue ferritin increased by 75% in HuH7 and 33% in H9C2. After treatment with 10 μM ELT for 8 hours, 85% ferritin reduction was seen in HuH7 and 46% in H9C2 cells (Figure 2C-D). Respective decrements in cellular iron were 25% in HuH7 and 65% in H9C2 cells. Thus, ELT decreased total cellular iron and cellular ferritin in both cell types, with ferritin decrements being proportionately greater in HuH7 than H9C2 cells. Thus, ferritin in HuH7 cells appears more responsive, both to iron loading and unloading than in H9C2 cells, consistent with the known higher iron storage capacity of hepatocytes.

ELT decreases ROS more rapidly than other chelators

Intracellular ROS generation by iron is predominantly determined by the LIP concentration.[31] Unlike measurement of total cellular iron or ferritin, continuous real-time measurement of ROS is achievable, allowing insight into kinetics of chelation. In Figure 3A-B, the ROS generation rate is rapidly decreased by ELT in HuH7 and H9C2 cells, even at the first measurable times. Inhibition of ROS by DFO was relatively slow, consistent with the known slow cellular uptake of DFO,[14] whereas DFP and DFX have intermediate effects. In Figure 3C-D, the inhibitory effects of 10 μM ELT and other chelators at 10 μM IBE (except CP40 at 33 μM IBE) are shown in HuH7, H9C2, and RINm5F cells. ROS generation is inhibited with ELT by 73% in HuH7 and by 61% in H9C2 cells, more than with other chelators at comparable concentrations. In Table 3 (top 4 rows), ROS inhibition at 1 μM is shown, where ELT has the greatest effect. Thus, rapid ROS decrements are similar both in hepatocytes and cardiomyocytes, unlike iron mobilization. The slower mobilization of total cellular iron will allow time for metabolic inactivation of ELT in hepatocytes, and hence decrease activity of ELT in these cells.

ELT decreases cellular iron and reverses iron-mediated suppression of insulin secretion in the pancreatic β-cell line (RINm5F)

After RINm5F cells were iron-loaded, 10 μM ELT subsequently mobilized a similar amount of iron to 10 μM IBE DFO or DFX at 8 hours (Figure 2E). ROS inhibition by ELT was found to be dose-sensitive, being greater at 10 μM ELT than 3 μM ELT (Figure 3E). When iron-loading was increased by increasing FBS from 10% to 25%, insulin secretion decreased (Figure 3F). Decrements in ROS and cellular iron were associated with restoration of insulin secretion (Figure 3G). This was also achieved with DFX, but not with DFO or DFP. Restoration of cell function is presumably related to decreasing ROS, secondary to lowering LIP.

Effects of chelator combinations with ELT on iron mobilization or ROS inhibition

Combinations of chelators may decrease the doses of individual chelators required for a given effect. When DFO, DFP, or DFX at 1 μM IBE were combined with 1 μM ELT, iron mobilization was greater than monotherapy with either ELT or a second chelator (Table 2, lower 3 rows). The most effective combination was ELT plus DFX, as it was greater than additive. However, ROS inhibition by ELT, when combined with other chelators, was never more than additive (Table 3, lower 3 rows). Iron mobilization using the combination of ELT (3 μM) with the extracellular chelator hydroxypyridinone chelator CP40 (3 μM) was also greater than additive (Figure 2F), suggesting entry of a second chelator into cells is not a prerequisite for synergistic chelation ("Discussion" and Figure 5C).

Mechanisms of synergistic iron removal by ELT when combined with DFX or CP40

In a cell-free system, ELT removed iron from preformed iron–citrate complexes (Figure 4A) faster than DFX (Figure 4B), suggesting ELT

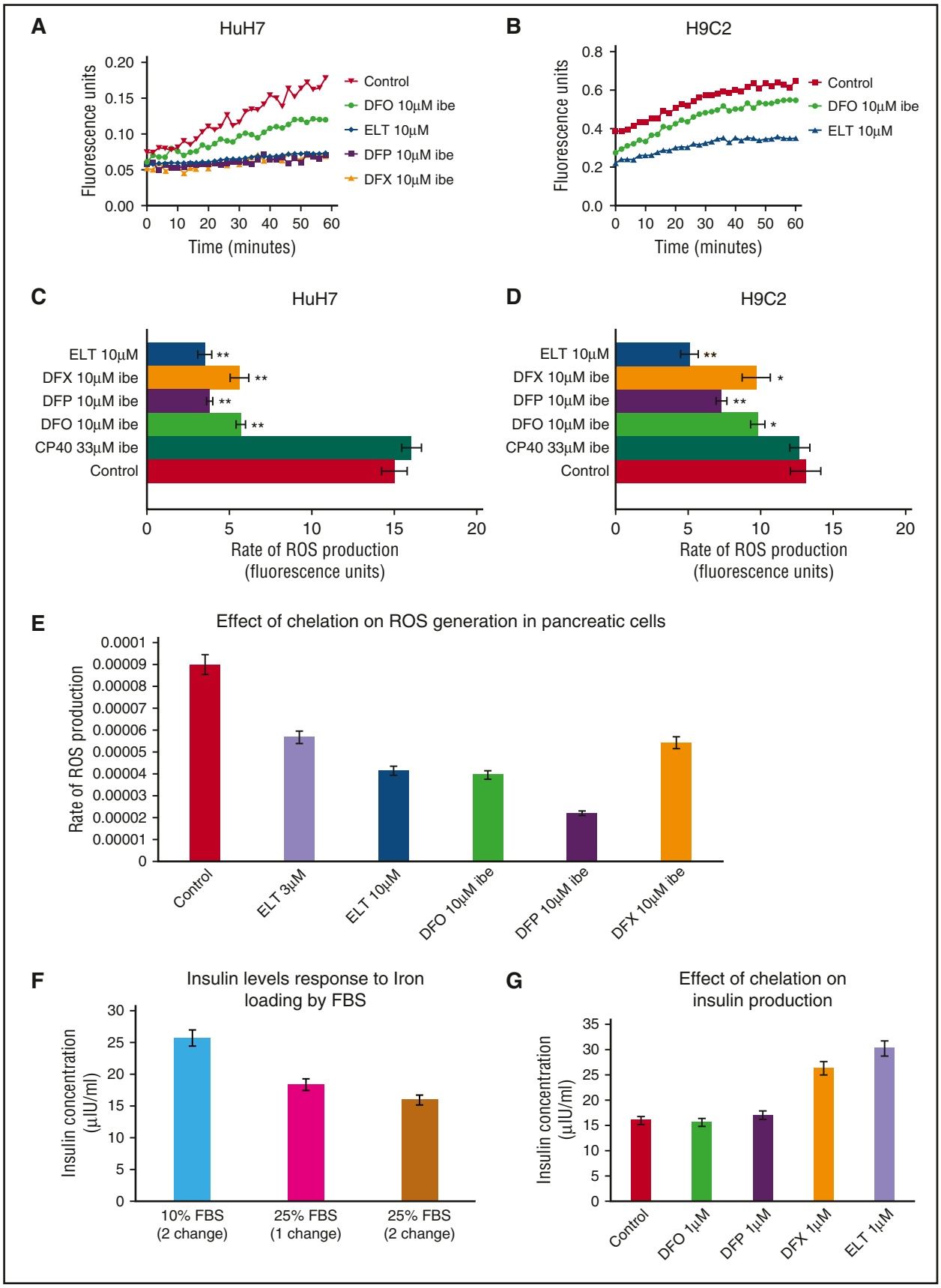

Figure 3. Effect of ELT and iron chelators on intracellular ROS generation and cell function (insulin production) in iron-loaded cells. The time-course for ROS inhibition by ELT and other chelators are shown in (A) HuH7 or (B) H9C2 cells. Cells were iron-loaded and then rinsed 4 times, as described earlier. Chelators were then added, and the rate of change of ROS production was recorded as fluorescence change (excitation at 504 nm, emission at 526 nm) continuously over the course of 1 hour in

Table 3. Comparison of ROS generation in cardiomyocyte (H9C2) and a hepatocyte (HuH7) cell lines is shown after addition of clinically available chelators or ELT, alone or in combination over the course of 90 minutes

	H9C2 cardiomyocyte-like cells	HuH7 hepatocyte-like cells
DFO 1 μM IBE	12.1 ± 1.3	14.3 ± 0.9
DFP 1 μM IBE	29.7 ± 1.3	25.0 ± 1.8
DFX 1 μM IBE	33.2 ± 2.7	21.4 ± 2.6
ELT 1 μM	42.2 ± 1.7	39.2 ± 2.1
ELT 1 μM + DFO 1 μM IBE	62.2 ± 3.2*	55.1 ± 3.1**
ELT 1 μM + DFP 1 μM IBE	60.3 ± 4.1*	60.2 ± 3.2*
ELT 1 μM + DFX 1 μM IBE	57.3 ± 3.3**	51.3 ± 2.2*

Experimental design and determination of ROS is otherwise as described in Figure 3. Results are the mean ± SEM of 4 observations in 1 experiment. (*$P < 0.05$, **$P < 0.01$ compared with control) percentage decrease in ROS generation rate at 90 minutes.

accesses some chelatable iron pools faster than DFX. Preformed complexes of ELT also donated iron to DFX (Figure 4C) or CP40 (Figure 4D) more rapidly than preformed ferric citrate complexes donated iron to DFX. Donation to DFX was most rapid at ELT:iron ratios of 2:1 or 3:1 (Figure 4E). Thus, ELT appears to satisfy the requirements of an iron shuttle,[32] capable of both rapid iron chelation as well as iron donation to a second chelator. As DFX is known to enter cells and chelate iron directly,[33] DFX could in principle act as a sink for chelated iron within the cells, which is unlikely with CP40.

Greater than additive chelation with DFX or CP40 could in principle also occur by inhibiting reuptake of iron from ELT complexes. In Figure 5A, ELT iron complexes donated iron to HuH7 cells. This was inhibited by the extracellular chelator CP40, but not by DFX (Figure 5A). However, DFX complexes can also donate iron to cells (Figure 5B), whereas CP40 does not.[34] This we attribute to the lipophilicity of DFX–iron complex, but the marked hydrophilicity of the CP40–iron complex.[11,12] Figure 5C suggests a mechanistic scheme for cellular iron mobilization by ELT alone, or combined with CP40. This involves cellular uptake of ELT and chelation of LIP, which we have not measured directly but is consistent with several lines of direct and indirect evidence (see "Discussion").

Discussion

We have demonstrated progressive removal of total cellular iron by ELT in H9C2, HuH7, and RINm5F cell lines. This is associated with lowering of intracellular ferritin, consistent with decrements in storage iron (although storage iron was not measured directly). This was also associated with decrements in ROS and with restoration of insulin secretion in iron-loaded RINm5F cells. In H9C2 cardiomyocyte-derived cells, ELT proved superior at mobilizing cellular iron to licensed iron chelators (DFO, DFP, and DFX) at a relatively low concentration. In the human hepatocellular HuH7 line, 1 μM ELT was less effective than in the rat cardiomyocyte H9C2 cell line (Table 2), but was increasingly effective at higher concentrations (Figure 2A). Rapid metabolism of ELT in HuH7 cells may decrease efficacy. ELT is metabolized by mono-oxygenation and glucuronidation, with liver conjugation preceding elimination in feces and urine.[35] Hepatocytes are typically more active in drug metabolism than cardiomyocytes, and HuH7 cells contain most of the phase 1 and phase 2 enzymes present in hepatocytes.[36] Thus, greater metabolic inactivation of ELT would be expected in HuH7 than H9C2 cells. Indeed, CYP2B1, 2B2, 2E1, and 2J3 are expressed at lower levels in H9C2 and myocardium than in hepatocytes.[32] As H9C2 cells are rat- rather than human-derived, interspecies differences in metabolism could contribute to the observed differences. In clinical use, however, metabolic inactivation of ELT is unlikely to be a major issue limiting iron chelation, as unmetabolized ELT accounts for more than 94% of drug at 4 hours, with 64% remaining unmetabolized at 24 hours.[35] The low ELT concentrations that are effective in cell culture may not necessarily translate to animal and clinical studies, particularly if metabolism, distribution, and elimination of iron complexes differ significantly in vivo. The effectiveness and doses of ELT required in vivo, alone or in combination with a second chelator, therefore need to be established.

Although we have not measured ELT entry into cells directly, we believe, based on several independent lines of evidence, that rapid cellular uptake of ELT is likely. First, ELT is taken up rapidly into isolated hepatocytes[37] and neuronal cells.[38] Second, studies with other chelators have shown that chelator entry into cells is key to cellular iron mobilization. The high lipophilicity and low molecular weight of ELT (Table 1) are properties associated with cellular uptake and high chelator efficacy.[11-14] Third, rapid ROS inhibition by ELT supports rapid cellular uptake. ROS inhibition appears to involve direct interaction of ELT with ROS,[4] which would require intracellular uptake by ELT. Fourth, ELT rapidly lowers labile intracellular iron,[3] the kinetics of which are more consistent with rapid ELT entry into cells than with secondary effects of iron depletion. Fifth, the lower cellular iron mobilization by ELT in HuH7 rather than H9C2 cells (contrasting with similar decrements in ROS) is consistent with greater metabolic inactivation in HuH7 cells, which itself requires intracellular access by ELT.

Our data show greater-than-additive cellular iron mobilization by combinations of ELT with either DFX or CP40, whereas additive effects are seen with DFO and DFP. Consideration of iron-binding constants (pFe) and speciation plots for these chelators (Table 1) suggested iron shuttling by ELT might account for the enhanced effects when combined with DFX or CP40. The phenomenon of iron shuttling has been described with other chelator combinations,[11,39-41] where 1 chelator possessing rapid access to iron pools subsequently donates iron to a sink chelator possessing greater stability for iron(III) binding, but slower kinetic access. In principle, a second chelator could act as a sink for iron chelated by ELT, either within or outside cells. Although the low molecular weight and lipophilicity of ELT, both as a free ligand and as iron complexes, are well suited to iron shuttling across cell membranes,[11] it is not essential for the sink chelator to enter cells for synergism to occur.[11] The donation of iron from ELT complexes to CP40 extracellularly could explain why CP40, which has no inherent iron mobilizing effects of its own because of its inability to enter cells, enhances iron chelation when combined with ELT. Indeed, this

Figure 3 (continued) the plate reader at 37°C. DFO, DFP, and DFX were used at 10 μM IBE, and ELT at 10 μM. The rate of ROS production was compared between chelator-treated and chelator-untreated cells. Data shown are readings from individual plates. ROS rate inhibition at 1 hour with CP40, DFO, DFP, DFX, and ELT is shown in (C) HuH7 and (D) H9C2 cells at 10 μM IBE for each chelator and 10 μM ELT and 33 μM IBE CP40. In both cell types, 10 μM ELT shows greater inhibition of ROS than other chelators at the same concentration in both HuH7 and H9C2 cells. The extracellular hydroxypyridinone chelator, CP40, had no effect on ROS. (E) Effect of chelator treatment during a 90-minute period in RINm5F cells on ROS generation is shown. Results are the mean ± SEM of 4 observations in 1 experiment. (F) Effect of iron loading in RINm5F cells with 2 changes of RPMI media containing 10% to 25% FBS on insulin secretion. After treatment, cells were challenged with Kreb's Ringer buffer containing glucose and insulin concentration in the supernatant determined as described in "Materials and methods." (G) Effect of chelation treatment on insulin production in RINm5F cells iron-loaded with two 10-hour changes of RPMI media containing 25% FBS. *$P < .05$; **$P < .01$ compared with control. Results are the mean ± SEM of 3 observations in 1 experiment.

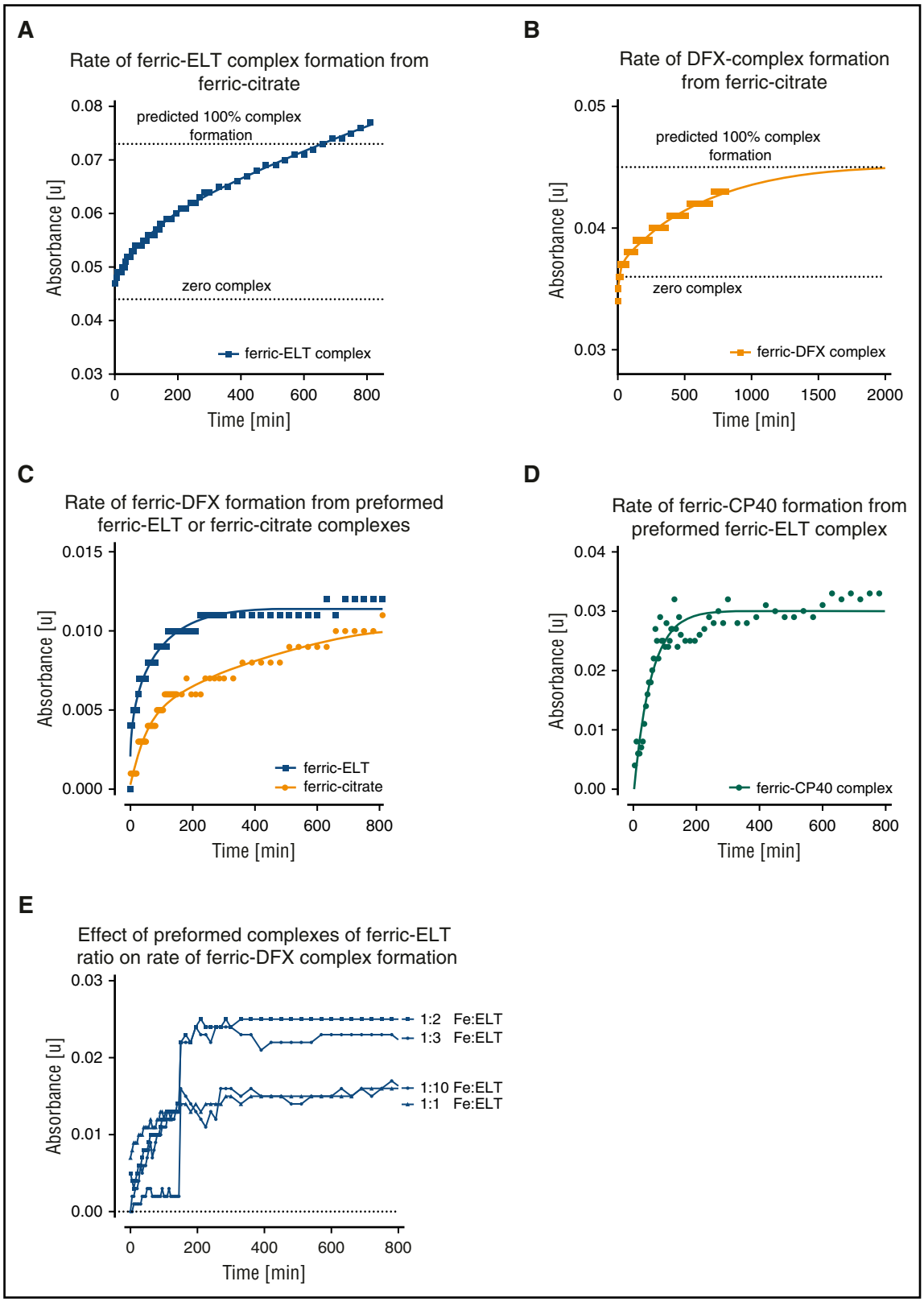

Figure 4. Rates of iron chelation and exchange between ELT and DFX in vitro. The rates of ferric–chelate complex formation from preformed ferric–citrate complexes (iron: citrate 10:100 μM) are shown with either (A) ELT (30 μM), monitored at 614 nm, which forms a secondary peak of ELT-Fe complex, or (B) DFX (30 μM), monitored at 556 nm, secondary peak for DFX-iron complex. The top horizontal line represents 100% iron complex formation of ELT or DFX (10 μM iron[III]). The lower horizontal lines represent the absorbances of the iron-free ligands (30 μM). It can be seen that ELT binds iron from ferric citrate complexes faster than DFX. The 50% effect is achieved at about 180 min for ELT, but later at around 300 min for DFX. The 100% effect is achieved by ELT at about 12 hours, whereas DFX takes approximately 33 hours. (C) The rates of ferric–DFX complex formation (300 μM of DFX) from either preformed ferric–citrate (iron:citrate 10:100 μM) or from ferric–ELT (10 μM, 1:2) is shown. It can be seen that DFX binds iron from preformed complexes of ELT faster than from ferric–citrate complexes (D). Rate of CP40 ferric complex formation is shown at 200 μM IBE CP40 from preformed 10 μM $FeELT_2$. The reaction is completed at approximately 200 minutes. (E) The effect of excess ELT ratio to iron on the rate of DFX chelation from preformed iron(III):ELT complexes (ratios 1:1, 1:2, 1:3, and 1:10) and 3.33, 6.66, 10, 33.3 μM ELT, respectively) are shown. Iron complexes of DFX form more rapidly and most completely when the ratio is 1:2 and 1:3 than with ratios of 1:1. A 10-fold excess of iron-free ELT to iron retards the rate of iron donation to DFX.

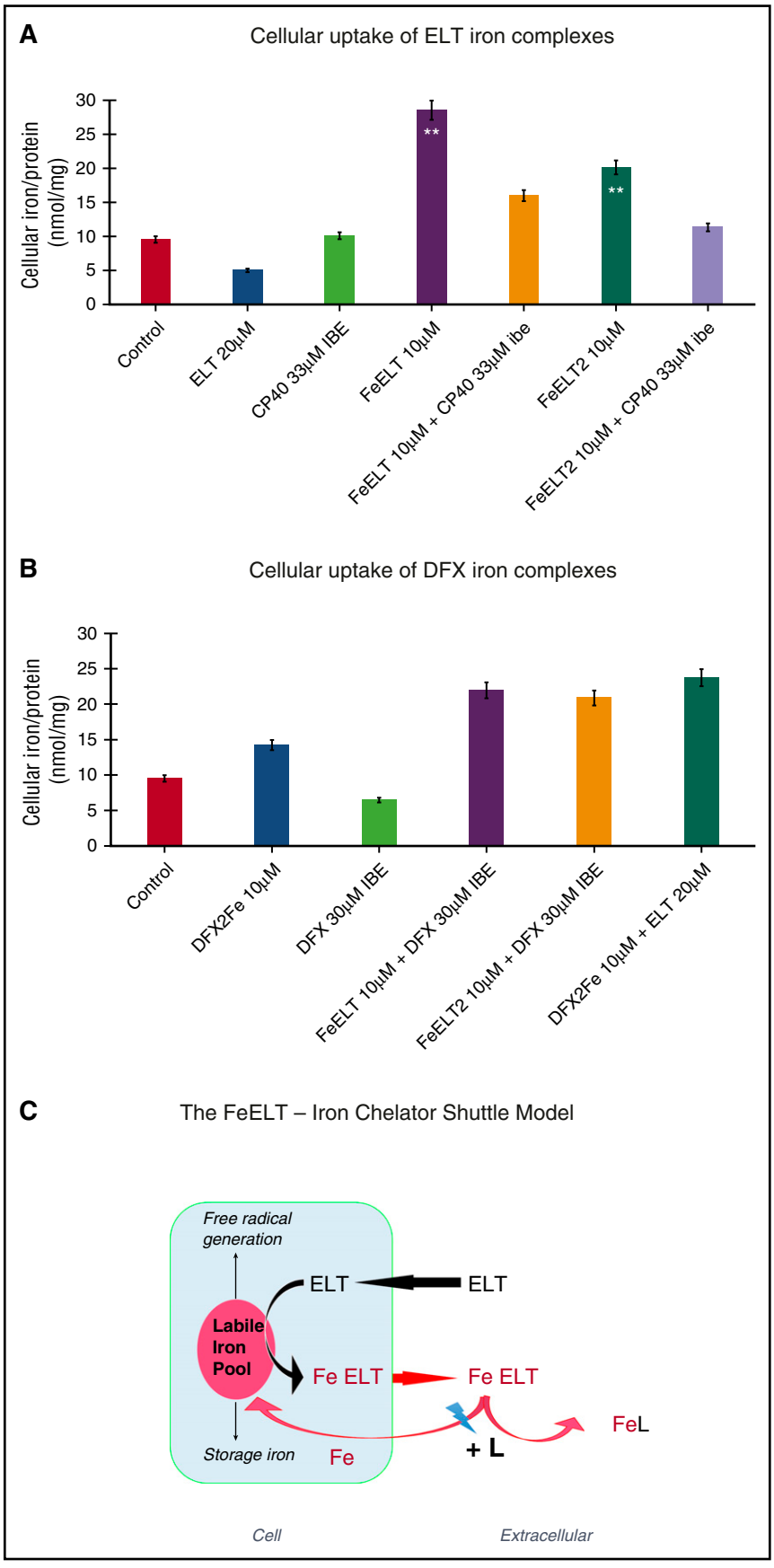

Figure 5. Cellular uptake of iron complexes of ELT, interactions with DFX and CP40, and proposed mechanisms of interaction of ELT with chelatable cellular iron and effects of second chelator. Iron uptake into HuH7 cells from preformed chelate complexes of ELT or DFX is shown at 6 hours in (A) and (B) of the same experiment. Control iron release with ELT or CP40 (A) or DFX alone (B) are also shown. CP40 was chosen for evaluation because of its lack of iron removal from cells when used as a single agent and its lack of iron donation to cells. After incubation, cells were washed, with the first wash containing DFO at 30 μM IBE and then with 3 PBS washes before intracellular iron concentration was determined, using the ferrozine assay as described in "Materials and methods." (A) Iron uptake from chelate complexes of ELT is shown, where complexes of ELT were presented either as 1:1 or 1:2 ratios of iron:ELT. CP40 inhibits iron uptake from both FeELT and FeELT2. (B) In contrast to CP40, DXF does not inhibit the net uptake of iron from preformed complexes of ELT. Preformed complexes of DFX (DFX2Fe) donate some iron to cells, but less than from complexes of ELT. (C) Proposed mechanisms of interaction of ELT with cellular iron with or without a second chelator. ELT diffuses into cells, rapidly binding LIP iron and thus decreasing ROS. Iron complexes of ELT then diffuse out of the cell, some of which can subsequently donate iron back to the cell (however establishing a net deironing effect of ELT monotherapy) (A). Diffusion of ELT into cells was not measured directly but has been previously shown in other cells and is consistent with its low molecular weight, its high lipid solubility, and rapid intracellular ROS inhibition. A second chelator (L) can increase intracellular iron chelation, and thus cellular iron release, if it gains direct access to LIP, as is known to occur with DFX, but not with CP40. ELT binds chelatable iron (from citrate) faster than DFX (Figure 4A-B). DFX binds iron from complexes of ELT faster than those bound to citrate (Fe:citrate 10:100) (Figure 4C). A second chelator can also increase net iron release extracellularly by competitive removal of iron from ELT–iron complexes, thus decreasing the donation of iron from ELT–iron complexes to cells. Both intracellular and extracellular donation of iron to a second chelator (L) potentially frees up ELT for a further round of iron chelation.

mechanism has been described with other iron chelators in combination with CP40.[11] Although the speciation plots in Figure 1B-E predict iron will eventually be donated by ELT onto DFX or DFO, they provide no direct evidence for the rate at which this occurs. We therefore undertook additional experiments in cell-free systems. ELT accessed citrate-bound iron faster than DFX (Figure 4A-B), which would accelerate net iron chelation, particularly if the iron was then donated to DFX as a shuttling effect. Indeed, we found iron donation from ELT complexes to DFX or CP40 at rates sufficient to account for enhanced chelation (Figure 4C-D). However, we also found that reuptake of iron from chelate–iron complexes needs to be accounted for. CP40 inhibited iron uptake from ELT complexes (Figure 5A), whereas DFX did not (Figure 5B). This may relate to DFX–iron complexes themselves being taken into cells (Figure 5B), unlike those of CP40. On the basis of these observations, and the speciation plot data, we have suggested an overall scheme for how greater-than-additive cellular iron removal may occur both extracellularly and intracellularly (Figure 5C). In this scheme, the greater-than-additive iron mobilization seen when CP40 was combined with ELT is mainly achieved extracellularly by CP40 (shown as L) accepting iron chelated by ELT, allowing ELT to become available for further iron chelation. The iron from the CP40–iron complex is not taken back up into cells, whereas iron can be donated by DFX complexes to cells (Figure 5B), and most of the greater-than-additive iron mobilization obtained by combining DFX (not shown) with ELT occurs intracellularly through accelerated chelation of LIP by ELT compared with DFX.

Our data are consistent with the iron-chelating effects of ELT being independent of the TPO-R effect because the latter is highly species-specific.[3,42] The thrombopoietic actions of ELT occur only in humans and primates, with no effect in rodents, whereas the iron mobilizing effects in our experiments were seen both in human HuH7 cells and rat H9C2 cardiomyocyte and RINm5f pancreatic cells. The chelating actions of ELT could be clinically beneficial in several settings. An obvious application would be the treatment of transfusional iron overload. The elimination route for iron complexes of ELT is currently unknown and requires studies in animal models and humans. Interspecies differences in metabolism and routes of elimination of iron complexes are well established with other chelators and may be unpredictable from first principles.[22] However, if iron chelated by ELT is donated to a second chelator such as DFX, the ELT iron complex would not need to be eliminated in urine or feces directly. This will need to be demonstrated in vivo, however.

In addition to increasing platelet counts, ELT can increase red cell and neutrophil counts and is approved in the United States for the treatment of severe aplastic anemia.[43] Some effects of ELT on hematopoiesis in myelodysplastic syndrome and aplastic anemia might be derived from this iron-chelating mechanism. As our data suggest that ELT–iron complexes can also donate iron to cells, iron redistribution should also be examined as a mechanism for improved hematopoiesis. Antileukemic effects mediated through modulation of intracellular iron content have also been postulated.[3] The antioxidant and iron chelation properties are tightly linked to cell death in leukemia cells,[3] as the antiproliferative and apoptotic effects of chelators are well described,[17,18] through mechanisms that include ribonucleotide reductase inhibition.[16] However, in patients with idiopathic thrombocytopenia, iron chelation could create or exacerbate iron deficiency, which needs to be explored. Importantly, the 1 μM ELT concentration that mobilized cellular iron is nearly twenty-fold less than peak plasma concentrations obtained after 30 mg ELT orally.[30] At this dose, platelet increments do not typically exceed 1.2 × baseline in healthy volunteers with repeat dosing.[44] Hence, in principle, effective chelating doses could be given without promoting unacceptable thrombocytosis, although requiring careful clinical study. In principle, still lower concentrations could be used when combined with a clinically licensed chelator. ELT has been generally well-tolerated long-term,[45] with the most common adverse events being headache, gastrointestinal symptoms, and upper respiratory tract infections.[45] Published studies did not demonstrate any correlation between ELT treatment and occurrence of thromboembolic events.[46-49] This suggests ELT doses that induced significant intracellular chelation could be administered to nonthrombocytopenic patients without appreciable changes in platelet counts.

In conclusion, we have demonstrated for the first time the iron-binding properties of ELT and its iron-mobilizing properties from cells in culture. Decrements in ROS and improved cell function were also observed. Single-agent ELT mobilized intracellular iron at concentrations similar to or lower than clinically licensed chelators, particularly from H9C2 cells. Additive or synergistic intracellular chelation with clinically available chelators has been shown. It will be important to demonstrate whether these in vitro effects and effective doses translate to iron-overloaded animals, and ultimately to the clinical setting.

Acknowledgments

We thank the Onassis Foundation, Athens, Greece, for their support in the form of a scholarship. J.P. is supported by the Biomedical Research Centre, University College London. J.P. and N.C have received honoraria for consultancy work and speaking at educational events sponsored by Novartis

Authorship

Contribution: E.V., Y.-L.C., M.G., B.P., M.S.-V., N.C., R.H., and J.P., designed research; E.V., Y.-L.C., M.G., and P.K. performed research; E.V., Y.-L.C., M.G., R.H., and J.P. analyzed and interpreted data; and E.V., Y.-L.C., R.H., and J.P. wrote the manuscript.

Conflict of interest disclosure: The authors declare no competing financial interests.

Correspondence: Evangelia Vlachodimitropoulou, Haematology Department, University College London, 3rd Floor, Paul O'Gorman Building, 72 Huntley St, London, WC1E 6BT United Kingdom; e-mail: evangelia.koumoutsea.11@ucl.ac.uk.

References

1. Williams DD, Peng B, Bailey CK, et al. Effects of food and antacids on the pharmacokinetics of eltrombopag in healthy adult subjects: two single-dose, open-label, randomized-sequence, crossover studies. *Clin Ther.* 2009;31(4): 764-776.
2. Wire MB, Bruce J, Gauvin J, et al. A randomized, open-label, 5-period, balanced crossover study to evaluate the relative bioavailability of eltrombopag powder for oral suspension (PfOS) and tablet formulations and the effect of a high-calcium meal on eltrombopag pharmacokinetics when administered with or 2 hours before or after PfOS. *Clin Ther.* 2012;34(3):699-709.
3. Roth M, Will B, Simkin G, et al. Eltrombopag inhibits the proliferation of leukemia cells via reduction of intracellular iron and induction of differentiation. *Blood.* 2012;120(2): 386-394
4. Kalota A, Selak MA, Garcia-Cid LA, Carroll M. Eltrombopag modulates reactive oxygen species and decreases acute myeloid leukemia cell survival. *PLoS One.* 2015;10(4): e0126691.

5. Kurokawa T, Murata S, Zheng YW, et al. The Eltrombopag antitumor effect on hepatocellular carcinoma. *Int J Oncol*. 2015;47(5):1696-1702.
6. Svensson T, Chowdhury O, Garelius H, et al. A pilot phase I dose finding safety study of the thrombopoietin-receptor agonist, eltrombopag, in patients with myelodysplastic syndrome treated with azacitidine. *Eur J Haematol*. 2014;93(5): 439-445.
7. Leitch HA, Vickars LM. Supportive care and chelation therapy in MDS: are we saving lives or just lowering iron? *Hematology Am Soc Hematol Educ Program*. 2009:664-672.
8. Olnes MJ, Scheinberg P, Calvo KR, et al. Eltrombopag and improved hematopoiesis in refractory aplastic anemia. *N Engl J Med*. 2012; 367(1):11-19.
9. Vlachodimitropoulou E, Cooper N, Psaila B, Sola-Visner M, Porter J. Eltrombopag mobilizes intracellular iron stores at concentrations lower than those required with other clinically available iron chelators [abstract]. *Blood*. 2014;124(21). Abstract 1353.
10. Vlachodimitropoulou E, Porter JB, Cooper N, Psaila B, Sola-Visner M.A potential novel application of eltrombopag: a combination agent to enhance iron chelation therapy [abstract]. *Blood*. 2015;126. Abstract 3357.
11. Vlachodimitropoulou Koumoutsea E, Garbowski M, Porter J. Synergistic intracellular iron chelation combinations: mechanisms and conditions for optimizing iron mobilization. *Br J Haematol*. 2015; 170(6):874-883.
12. Porter JB, Gyparaki M, Burke LC, et al. Iron mobilization from hepatocyte monolayer cultures by chelators: the importance of membrane permeability and the iron-binding constant. *Blood*. 1988;72(5):1497-1503.
13. Porter JB, Morgan J, Hoyes KP, Burke LC, Huehns ER, Hider RC. Relative oral efficacy and acute toxicity of hydroxypyridin-4-one iron chelators in mice. *Blood*. 1990;76(11):2389-2396.
14. Hoyes KP, Porter JB. Subcellular distribution of desferrioxamine and hydroxypyridin-4-one chelators in K562 cells affects chelation of intracellular iron pools. *Br J Haematol*. 1993; 85(2):393-400.
15. Cooper CE, Lynagh GR, Hoyes KP, Hider RC, Cammack R, Porter JB. The relationship of intracellular iron chelation to the inhibition and regeneration of human ribonucleotide reductase. *J Biol Chem*. 1996;271(34):20291-20299.
16. Kayyali R, Porter JB, Liu ZD, et al. Structure-function investigation of the interaction of 1- and 2-substituted 3-hydroxypyridin-4-ones with 5-lipoxygenase and ribonucleotide reductase. *J Biol Chem*. 2001;276(52):48814-48822.
17. Hoyes KP, Hider RC, Porter JB. Cell cycle synchronization and growth inhibition by 3-hydroxypyridin-4-one iron chelators in leukemia cell lines. *Cancer Res*. 1992;52(17):4591-4599.
18. Maclean KH, Cleveland JL, Porter JB. Cellular zinc content is a major determinant of iron chelator-induced apoptosis of thymocytes. *Blood*. 2001;98(13):3831-3839.
19. Porter J, Hershko C. The properties of clinically useful iron chelators iron phyisology and pathophysiology in humans. In: Anderson HJ, McLaren GD, eds. New York: Humana Press; 2012:591-630.
20. Ma Y, Kong X, Chen Y-l, Hider RC. Synthesis and characterizations of pyridazine-based iron chelators. *Dalton Trans*. 2014;43(45): 17120-17128.
21. Porter JB, Singh S, Hoyes KP, Epemolu O, Abeysinghe RD, Hider RC. Lessons from preclinical and clinical studies with 1,2-diethyl-3-hydroxypyridin-4-one, CP94 and related compounds. *Adv Exp Med Biol*. 1994;356: 361-370.
22. Porter JB, Abeysinghe RD, Hoyes KP, et al. Contrasting interspecies efficacy and toxicology of 1,2-diethyl-3-hydroxypyridin-4-one, CP94, relates to differing metabolism of the iron chelating site. *Br J Haematol*. 1993;85(1):159-168.
23. Gans P, O'Sullivan B. GLEE, a new computer program for glass electrode calibration. *Talanta*. 2000;51(1):33-37.
24. Gans P, Sabatini A, Vacca A. Determination of equilibrium constants from spectrophometric data obtained from solutions of known pH: the program pHab. *Ann Chim*. 1999;89:45-49.
25. Alderighi L, Gans P, Ienco A, Peters D, Sabatini A, Vacca A. Hyperquad simulation and speciation (HySS): a utility program for the investigation of equilibria involving soluble and partially soluble species. *Coord Chem Rev*. 1999;184(1):311-318.
26. Evans RW, Rafique R, Zarea A, et al. Nature of non-transferrin-bound iron: studies on iron citrate complexes and thalassemic sera. *J Biol Inorg Chem*. 2008;13(1):57-74.
27. Lu TH, Su CC, Chen YW, et al. Arsenic induces pancreatic β-cell apoptosis via the oxidative stress-regulated mitochondria-dependent and endoplasmic reticulum stress-triggered signaling pathways. *Toxicol Lett*. 2011;201(1):15-26.
28. Praz GA, Halban PA, Wollheim CB, Blondel B, Strauss AJ, Renold AE. Regulation of immunoreactive-insulin release from a rat cell line (RINm5F). *Biochem J*. 1983;210(2):345-352.
29. Cheminformatics on the Web. Available at www.molinspiration.com.
30. Gibiansky E, Zhang J, Williams D, Wang Z, Ouellet D. Population pharmacokinetics of eltrombopag in healthy subjects and patients with chronic idiopathic thrombocytopenic purpura. *J Clin Pharmacol*. 2011;51(6):842-856.
31. Cabantchik ZI. Labile iron in cells and body fluids: physiology, pathology, and pharmacology. *Front Pharmacol*. 2014;5:45.
32. Zordoky BN, El-Kadi AO. H9c2 cell line is a valuable in vitro model to study the drug metabolizing enzymes in the heart. *J Pharmacol Toxicol Methods*. 2007;56(3):317-322.
33. Glickstein H, El RB, Link G, et al. Action of chelators in iron-loaded cardiac cells: Accessibility to intracellular labile iron and functional consequences. *Blood*. 2006;108(9):3195-3203.
34. Garbowski MWEP, Evans P, Vlachodimitropoulou E, Hider R, Porter JB. Residual erythropoiesis protects against myocardial hemosiderosis in transfusion-dependent thalassemia by lowering labile plasma iron via transient generation of apotransferrin [published online ahead of print 22 June 2017]. *Haematologica*. doi: 10.3324/haematol.2017.170605.
35. Deng Y, Madatian A, Wire MB, et al. Metabolism and disposition of eltrombopag, an oral, nonpeptide thrombopoietin receptor agonist, in healthy human subjects. *Drug Metab Dispos*. 2011;39(9):1734-1746.
36. Guo L, Dial S, Shi L, et al. Similarities and differences in the expression of drug-metabolizing enzymes between human hepatic cell lines and primary human hepatocytes. *Drug Metab Dispos*. 2011;39(3):528-538.
37. Takeuchi K, Sugiura T, Umeda S, et al. Pharmacokinetics and hepatic uptake of eltrombopag, a novel platelet-increasing agent. *Drug Metab Dispos*. 2011;39(6):1088-1096.
38. Bastian TW, Duck KA, Michalopoulos GC, et al. Eltrombopag, a thrombopoietin mimetic, crosses the blood-brain barrier and impairs iron-dependent hippocampal neuron dendrite development. *J Thromb Haemost*. 2017;15(3): 565-574.
39. Srichairatanakool S, Kemp P, Porter JB. Evidence for "shuttle" effect of NTBI onto desferrioxamine in thalassaemic plasma in the presence of NTA. In: International Symposium: Iron in Biology and Medicine; 1997; St. Malo, France.
40. Giardina PJ, Grady RW. Chelation therapy in beta-thalassemia: an optimistic update. *Semin Hematol*. 2001;38(4):360-366.
41. Evans P, Kayyali R, Hider RC, Eccleston J, Porter JB. Mechanisms for the shuttling of plasma non-transferrin-bound iron (NTBI) onto deferoxamine by deferiprone. *Transl Res*. 2010;156(2):55-67.
42. Erickson-Miller CL, Delorme E, Tian SS, et al. Preclinical activity of eltrombopag (SB-497115), an oral, nonpeptide thrombopoietin receptor agonist. *Stem Cells*. 2009;27(2):424-430.
43. Design iW. eltrombopag (Revolade (EU), Promacta (US)) UKMi New Drugs Online Database. 2016.
44. Jenkins JM, Williams D, Deng Y, et al. Phase 1 clinical study of eltrombopag, an oral, nonpeptide thrombopoietin receptor agonist. *Blood*. 2007; 109(11):4739-4741.
45. Saleh MN, Bussel JB, Cheng G, et al; EXTEND Study Group. Safety and efficacy of eltrombopag for treatment of chronic immune thrombocytopenia: results of the long-term, open-label EXTEND study. *Blood*. 2013;121(3): 537-545.
46. Bussel JB, Cheng G, Saleh MN, et al. Eltrombopag for the treatment of chronic idiopathic thrombocytopenic purpura. *N Engl J Med*. 2007;357(22):2237-2247.
47. Bussel JB, Provan D, Shamsi T, et al. Effect of eltrombopag on platelet counts and bleeding during treatment of chronic idiopathic thrombocytopenic purpura: a randomised, double-blind, placebo-controlled trial. *Lancet*. 2009; 373(9664):641-648.
48. Bussel JB, Saleh MN, Vasey SY, Mayer B, Arning M, Stone NL. Repeated short-term use of eltrombopag in patients with chronic immune thrombocytopenia (ITP). *Br J Haematol*. 2013; 160(4):538-546.
49. Cheng G, Saleh MN, Marcher C, et al. Eltrombopag for management of chronic immune thrombocytopenia (RAISE): a 6-month, randomised, phase 3 study. *Lancet*. 2011; 377(9763):393-402.
50. Martell A. The design and synthesis of chelating agents. In: Martell AE, Anderson WF, Badman DG, eds. Development of Iron Chelators for Clinical Use. North-Holland, Amsterdam: Elsevier; 1981.
51. Ihnat PM, Vennerstrom JL, Robinson DH. Solution equilibria of deferoxamine amides. *J Pharm Sci*. 2002;91(7):1733-1741.
52. Motekaitis R, Martell A. Stabilities of the iron(III) chelates of 1,2-dimethyl-3-hydroxy-4-pyridinone and related ligands. *Inorg Chim Acta*. 1991; 183(1):71-80.
53. Nick H, Wong A, Acklin P, et al. ICL670A: preclinical profile. *Adv Exp Med Biol*. 2002;509: 185-203.